

# Modeling and Design of Level Inverter for Grid-Connected PV Fed Induction Motor Drive

Sakinala Govardhan

Assistant Professor, Department of EEE, CITS –Warangal.

**Abstract:** Photovoltaic power generation employs solar panels composed of a number of solar cells containing a photovoltaic material. Multilevel inverter structures have been developed to overcome shortcomings in solid-state switching device ratings so that they can be applied to high voltage electrical systems. The multilevel voltage source inverters unique structure allows them to reach high voltages with low harmonics without the use of transformers. This makes unique power electronics topologies suitable for Flexible AC Transmission Systems and custom power applications. The use of a multilevel converter to control the frequency, voltage output including phase angle, real and reactive power flow at a dc/ac interface provides significant opportunities in the control of distributed power systems. In this concept, new system architecture for 7-level MLI system is proposed. This method allows the renewable energy sources to deliver the load together or independently depending upon their availability. The proposed inverter uses less number of switches when compared with the conventional multilevel inverter. This concept can be extended to apply for induction motor drive i.e., a 3-Phase Seven Level Inverter for Grid connected PV system fed Induction Motor Drive.

**Key Words:** Grid connected, modulation index, multilevel inverter, photovoltaic (PV) system, pulse width-modulated (PWM), Total Harmonic Distortion (THD), Induction Motor.

## I. INTRODUCTION

Nowadays renewable energy generation systems are gaining more attraction due to the exhaustive nature of fossil fuel resources and its increased prices. Also the need for pollution free green energy has created a keen interest towards alternate energy sources. Solar power is the most common and available renewable power source to meet our rapidly increasing energy requirements [1]. Peak power from the solar PV module is to be tracked for its efficient implementation. Various algorithms are available in the literature for tracking maximum power from solar panels. In this paper Perturbation and Observation algorithm is considered due to its simplicity. A boost converter is used to implement maximum power point tracking algorithm [2]. The output power generated from the solar panels is intermittent in nature and varies with the irradiance level. Hence to make the system more reliable, a battery is included in the system. A bidirectional converter is also used to adjust the flow of power from and into the battery [3]. A seven level inverter is used to convert the dc voltage from the solar

PV array to ac voltage and connect feed to the load. In this paper a novel topology for three phase seven level inverter is suggested [4]. This topology uses reduced number of switches compared to conventional seven level inverter topologies. Multilevel inverters produce a desired output voltage from different levels of direct current voltages as inputs.

As the number of levels increases, the synthesized output waveform is staircase wave which approximates a sine wave with more number of steps. Thus the output voltage approaches the desired sinusoidal waveform [5]. The basic idea of a multilevel converter is to obtain higher operating voltage using a series connection of power semiconductor switches with much lower voltage rating compared to power switches used in conventional two-level inverter. These power switches are controlled in such a way that more number of voltage levels is generated in the output using many dc sources. The rated voltage of the power semiconductor switches depends upon the rating of the input voltage sources to which they are connected and it is much less than the output voltage [6]. The main advantages of a multilevel inverter are that they can generate the output voltages with very less THD, can draw input current with very low distortion, lower EMI effects, and lower dv/dt across each switch and can operate at wide range of switching frequencies from fundamental frequency to very high frequency. The most common topologies for multilevel inverters are diode clamped, flying capacitor and cascaded H- bridge multilevel inverter. This paper was applied to three phase asynchronous machine photovoltaic system with considerations for voltage control pulse generator [7-10].

## II. PROPOSED MULTILEVEL INVERTER TOPOLOGY

The proposed single-phase seven-level inverter was developed from the five-level inverter in [25]–[29]. It comprises a single-phase conventional H-bridge inverter, two bidirectional switches, and a capacitor voltage divider formed by  $C_1$ ,  $C_2$ , and  $C_3$ , as shown in Fig.1. The modified H-bridge topology is significantly advantageous over other topologies, i.e., less power switch, power diodes, and less capacitors for inverters of the same number of levels.

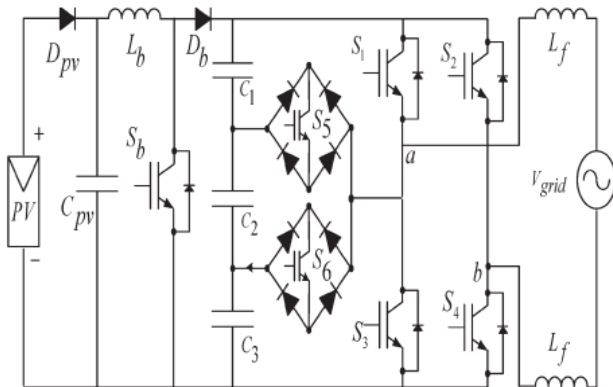


Fig.1. Proposed single-phase seven-level grid-connected inverter for photovoltaic systems.

Photovoltaic (PV) arrays were connected to the inverter via a dc–dc boost converter. The power generated by the inverter is to be delivered to the power network, so the utility grid, rather than a load, was used. The dc–dc boost converter was required because the PV arrays had a voltage that was lower than the grid voltage. High dc bus voltages are necessary to ensure that power flows from the PV arrays to the grid. A filtering inductance  $L_f$  was used to filter the current injected into the grid. Proper switching of the inverter can produce seven output-voltage levels ( $V_{dc}$ ,  $2V_{dc}/3$ ,  $V_{dc}/3$ ,  $0$ ,  $-V_{dc}$ ,  $-2V_{dc}/3$ ,  $-V_{dc}/3$ ) from the dc supply voltage.

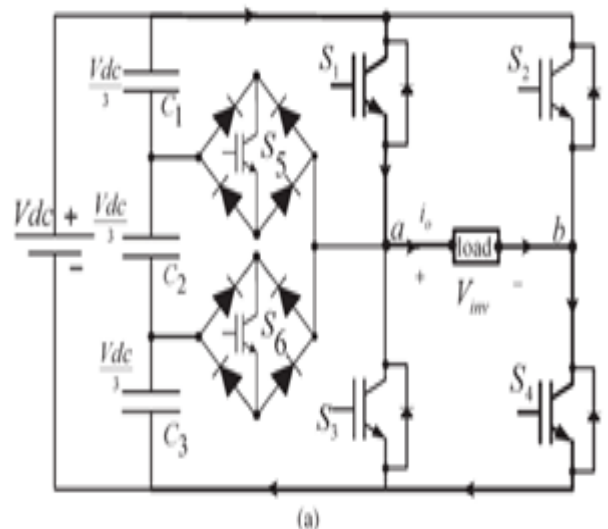
The proposed inverter's operation can be divided into seven switching states, as shown in Fig.3.2 (a)–(g). Fig.3.2 (a), (d), and (g) shows a conventional inverter's operational states in sequence, while Fig.3.2 (b), (c), (e), and (f) shows additional states in the proposed inverter synthesizing one- and two-third levels of the dc-bus voltage.

The required seven levels of output voltage were generated as follows.

1. Maximum positive output ( $V_{dc}$ ): S1 is ON, connecting the load positive terminal to  $V_{dc}$ , and S4 is ON, connecting the load negative terminal to ground. All other controlled switches are OFF; the voltage applied to the load terminals is  $V_{dc}$ . Fig.3.2 (a) shows the current paths that are active at this stage.
2. Two-third positive output ( $2V_{dc}/3$ ): The bidirectional switch S5 is ON, connecting the load positive terminal, and S4 is ON, connecting the load negative terminal to ground. All other controlled switches are OFF; the voltage applied to the load terminals is  $2V_{dc}/3$ . Fig.3.2 (b) shows the current paths that are active at this stage.
3. One-third positive output ( $V_{dc}/3$ ): The bidirectional switch S6 is ON, connecting the load positive terminal, and S4 is ON, connecting the load negative terminal to ground. All other

controlled switches are OFF; the voltage applied to the load terminals is  $V_{dc}/3$ . Fig.3.2 (c) shows the current paths that are active at this stage.

4. Zero output: This level can be produced by two switching combinations; switches S3 and S4 are ON, or S1 and S2 are ON, and all other controlled switches are OFF; terminal ab is a short circuit, and the voltage applied to the load terminals is zero. Fig.3.2 (d) shows the current paths that are active at this stage.
5. One-third negative output ( $-V_{dc}/3$ ): The bidirectional switch S5 is ON, connecting the load positive terminal, and S2 is ON, connecting the load negative terminal to  $V_{dc}$ . All other controlled switches are OFF; the voltage applied to the load terminals is  $-V_{dc}/3$ . Fig.3.2 (e) shows the current paths that are active at this stage.
6. Two-third negative output ( $-2V_{dc}/3$ ): The bidirectional switch S6 is ON, connecting the load positive terminal, and S2 is ON, connecting the load negative terminal to ground. All other controlled switches are OFF; the voltage applied to the load terminals is  $-2V_{dc}/3$ . Fig.3.2 (f) shows the current paths that are active at this stage.
7. Maximum negative output ( $-V_{dc}$ ): S2 is ON, connecting the load negative terminal to  $V_{dc}$ , and S3 is ON, connecting the load positive terminal to ground. All other controlled switches are OFF; the voltage applied to the load terminals is  $-V_{dc}$ . Fig.3.2 (g) shows the current paths that are active at this stage.



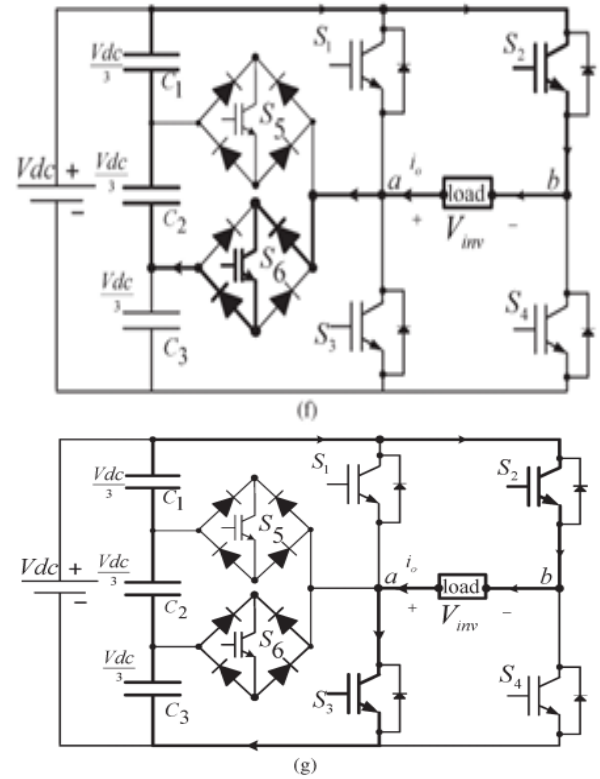
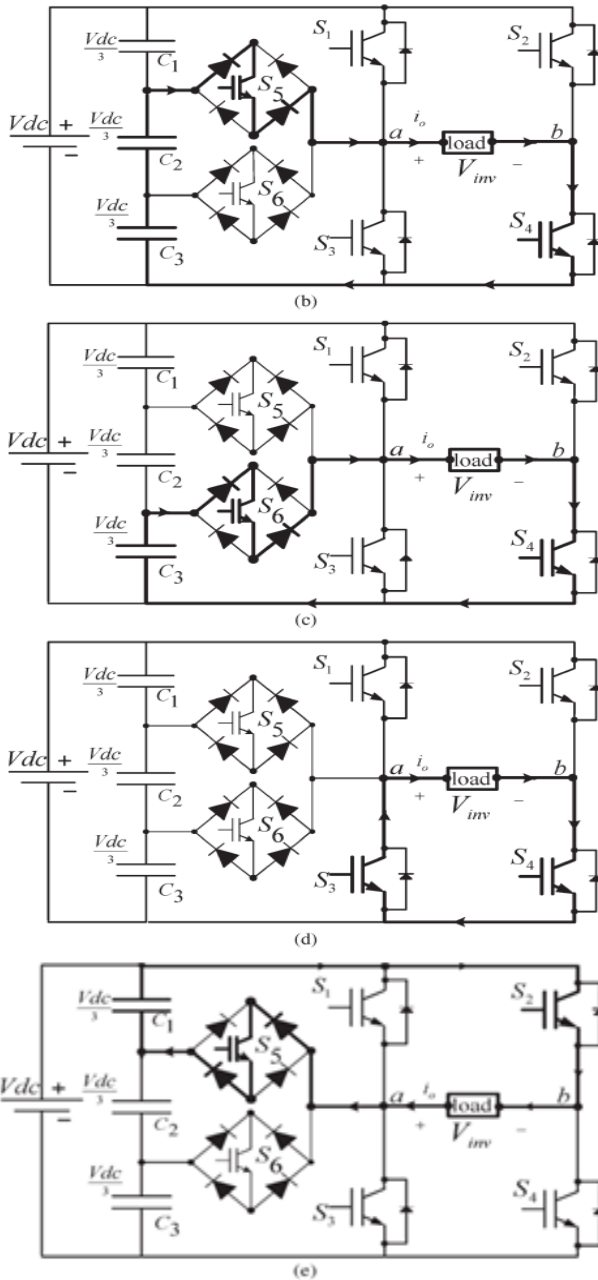


Fig.2. Switching combination required to generate the output voltage ( $V_{ab}$ ).  
(a)  $V_{ab} = V_{dc}$ . (b)  $V_{ab} = 2V_{dc}/3$ . (c)  $V_{ab} = V_{dc}/3$ . (d)  $V_{ab} = 0$ . (e)  $V_{ab} = -V_{dc}/3$ .  
(f)  $V_{ab} = -2V_{dc}/3$ . (g)  $V_{ab} = -V_{dc}$ .

Table.1 shows the switching combinations that generated the seven output-voltage levels ( $0, -V_{dc}, -2V_{dc}/3, -V_{dc}/3, V_{dc}, 2V_{dc}/3, V_{dc}/3$ ).

Table.1

Output Voltage According To the Switches' On-Off Condition

$v_0$	$S_1$	$S_2$	$S_3$	$S_4$	$S_5$	$S_6$
$V_{dc}$	on	off	off	on	off	off
$2V_{dc}/3$	off	off	off	on	on	off
$V_{dc}/3$	off	off	off	on	off	on
0	off	off	on	on	off	off
0*	on	on	off	off	off	off
$-V_{dc}/3$	off	on	off	off	on	off
$-2V_{dc}/3$	off	on	off	off	off	on
$-V_{dc}$	off	on	on	off	off	off

### III. PWM MODULATION

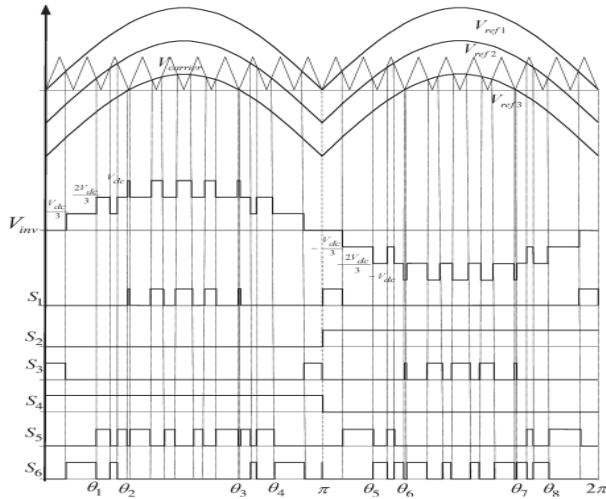


Fig.3. Switching pattern for the single-phase seven-level inverter.

A novel PWM modulation technique was introduced to generate the PWM switching signals. Three reference signals ( $V_{ref1}$ ,  $V_{ref2}$ , and  $V_{ref3}$ ) were compared with a carrier signal ( $V_{carrier}$ ). The reference signals had the same frequency and amplitude and were in phase with an offset value that was equivalent to the amplitude of the carrier signal. The reference signals were each compared with the carrier signal. If  $V_{ref1}$  had exceeded the peak amplitude of  $V_{carrier}$ ,  $V_{ref2}$  was compared with  $V_{carrier}$  until it had exceeded the peak amplitude of  $V_{carrier}$ . Then, onward,  $V_{ref3}$  would take charge and would be compared with  $V_{carrier}$  until it reached zero. Once  $V_{ref3}$  had reached zero,  $V_{ref2}$  would be compared until it reached zero. Then, onward,  $V_{ref1}$  would be compared with  $V_{carrier}$ . Fig.3 shows the resulting switching pattern. Switches  $S_1$ ,  $S_3$ ,  $S_5$ , and  $S_6$  would be switching at the rate of the carrier signal frequency, whereas  $S_2$  and  $S_4$  would operate at a frequency that was equivalent to the fundamental frequency.

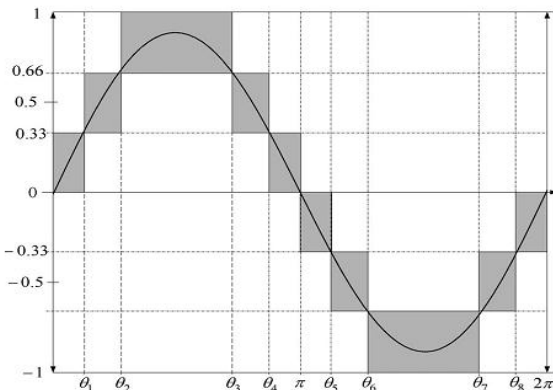


Fig.4. Seven-level output voltage ( $V_{ab}$ ) and switching angles.

For one cycle of the fundamental frequency, the proposed inverter operated through six modes. Fig.4 shows the per unit output-voltage signal for one cycle. The six modes are described as follows:

- Mode 1 :  $0 < \omega t < \theta_1$  and  $\theta_4 < \omega t < \pi$
- Mode 2 :  $\theta_1 < \omega t < \theta_2$  and  $\theta_3 < \omega t < \theta_4$
- Mode 3 :  $\theta_2 < \omega t < \theta_3$
- Mode 4 :  $\pi < \omega t < \theta_5$  and  $\theta_8 < \omega t < 2\pi$
- Mode 5 :  $\theta_5 < \omega t < \theta_6$  and  $\theta_7 < \omega t < \theta_8$
- Mode 6 :  $\theta_6 < \omega t < \theta_7$ .

(1)

The phase angle depends on modulation index  $M_a$ . Theoretically, for a single reference signal and a single carrier signal, the modulation index is defined to be

$$M_a = \frac{A_m}{A_c} \quad (2)$$

While for a single-reference signal and a dual carrier signal, the modulation index is defined to be [26]–[29]

$$M_a = \frac{A_m}{2A_c} \quad (3)$$

Since the proposed seven-level PWM inverter utilizes three carrier signals, the modulation index is defined to be

$$M_a = \frac{A_m}{3A_c} \quad (4)$$

Where  $A_c$  is the peak-to-peak value of the carrier signal and  $A_m$  is the peak value of the voltage reference signal  $V_{ref}$ .

When the modulation index is less than 0.33, the phase angle displacement is

$$\theta_1 = \theta_2 = \theta_3 = \theta_4 = \frac{\pi}{2} \quad (5)$$

$$\theta_5 = \theta_6 = \theta_7 = \theta_8 = \frac{3\pi}{2} \quad (6)$$

On the other hand, when the modulation index is more than 0.33 and less than 0.66, the phase angle displacement is determined by

$$\theta_1 = \sin^{-1} \left( \frac{A_c}{A_m} \right) \quad (7)$$

$$\theta_2 = \theta_3 = \frac{\pi}{2} \quad (8)$$

$$\theta_4 = \pi - \theta_1 \quad (9)$$

$$\theta_5 = \pi + \theta_1 \quad (10)$$

$$\theta_6 = \theta_7 = \frac{3\pi}{2} \quad (11)$$

$$\theta_8 = 2\pi - \theta_1. \quad (12)$$

If the modulation index is more than 0.66, the phase angle displacement is determined by

$$\theta_1 = \sin^{-1} \left( \frac{A_c}{A_m} \right) \quad (13)$$

$$\theta_2 = \sin^{-1} \left( \frac{2A_c}{A_m} \right) \quad (14)$$

$$\theta_3 = \pi - \theta_2 \quad (15)$$

$$\theta_4 = \pi - \theta_1 \quad (16)$$

$$\theta_5 = \pi + \theta_1 \quad (17)$$

$$\theta_6 = \pi + \theta_2 \quad (18)$$

$$\theta_7 = 2\pi - \theta_2 \quad (19)$$

$$\theta_8 = 2\pi - \theta_1 \quad (20)$$

For  $M_a$  that is equal to, or less than, 0.33, only the lower reference wave ( $V_{ref3}$ ) is compared with the triangular carrier signal. The inverter's behavior is similar to that of a conventional full-bridge three-level PWM inverter. However, if  $M_a$  is more than 0.33 and less than 0.66, only  $V_{ref2}$  and  $V_{ref3}$  reference signals are compared with the triangular carrier wave. The output voltage consists of five dc-voltage levels. The modulation index is set to be more than 0.66 for seven levels of output voltage to be produced. Three reference signals have to be compared with the triangular carrier signal to produce switching signals for the switches.

#### IV. CONTROL SYSTEM

As Fig.5 shows, the control system comprises a MPPT algorithm, a dc-bus voltage controller, reference-current generation, and a current controller. The two main

tasks of the control system are maximization of the energy transferred from the PV arrays to the grid, and generation of a sinusoidal current with minimum harmonic distortion, also under the presence of grid voltage harmonics.

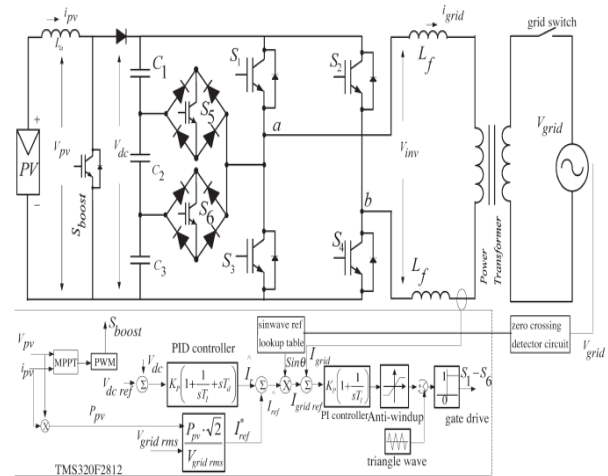


Fig.5. Seven-level inverter with closed-loop control algorithm.

The proposed inverter utilizes the perturb-and-observe (P&O) algorithm for its wide usage in MPPT owing to its simple structure and requirement of only a few measured parameters. It periodically perturbs (i.e., increment or decrement) the array terminal voltage and compares the PV output power with that of the previous perturbation cycle. If the power was increasing, the perturbation would continue in the same direction in the next cycle; otherwise, the direction would be reversed. This means that the array terminal voltage is perturbed every MPPT cycle; therefore, when the MPP is reached, the P&O algorithm will oscillate around it.

The P&O algorithm was implemented in the dc-dc boost converter. The output of the MPPT is the duty-cycle function. As the dc-link voltage  $V_{dc}$  was controlled in the dc-ac seven level PWM inverter, the change of the duty cycle changes the voltage at the output of the PV panels. A PID controller was implemented to keep the output voltage of the dc-dc boost converter ( $V_{dc}$ ) constant by comparing  $V_{dc}$  and  $V_{dc\ ref}$  and feeding the error into the PID controller, which subsequently tries to reduce the error. In this way, the  $V_{dc}$  can be maintained at a constant value and at more than  $\sqrt{2}$  of  $V_{grid}$  to inject power into the grid.

To deliver energy to the grid, the frequency and phase of the PV inverter must equal those of the grid; therefore, a grid synchronization method is needed. The sine lookup table that generates reference current must be brought into phase with the grid voltage ( $V_{grid}$ ). For this, the grid period and phase must be detected.

The proposed inverter provides an analog zero-crossing detection circuit on one of its input ports where the grid voltage is to be connected. The zero-crossing circuit then produces an in-phase square-wave output that is fed into the digital I/O port on eZdsp board TMS320F2812.

A PI algorithm was used as the feedback current controller for the application. The current injected into the grid, also known as grid current  $I_{grid}$ , was sensed and fed back to a comparator that compared it with the reference current  $I_{gridref}$ .  $I_{gridref}$  is the result of the MPPT algorithm. The error from the comparison process of  $I_{grid}$  and  $I_{gridref}$  was fed into the PI controller. The output of the PI controller, also known as  $V_{ref}$ , goes through an anti-wind up process before being compared with the triangular wave to produce the switching signals for  $S_1 - S_6$ . Eventually,  $V_{ref}$  becomes  $V_{ref1}$ ;  $V_{ref2}$  and  $V_{ref3}$  can be derived from  $V_{ref1}$  by shifting the offset value, which was equivalent to the amplitude of the triangular wave. The mathematical formulation of the PI algorithm and its implementation in the DSP are discussed in detail in [28].

## V. INDUCTION MOTOR

An asynchronous motor type of an induction motor is an AC electric motor in which the electric current in the rotor needed to produce torque is obtained by electromagnetic induction from the magnetic field of the stator winding. An induction motor can therefore be made without electrical connections to the rotor as are found in universal, DC and synchronous motors. An asynchronous motor's rotor can be either wound type or squirrel-cage type.

Three-phase squirrel-cage asynchronous motors are widely used in industrial drives because they are rugged, reliable and economical. Single-phase induction motors are used extensively for smaller loads, such as household appliances like fans. Although traditionally used in fixed-speed service, induction motors are increasingly being used with variable-frequency drives (VFDs) in variable-speed service. VFDs offer especially important energy savings opportunities for existing and prospective induction motors in variable-torque centrifugal fan, pump and compressor load applications. Squirrel cage induction motors are very widely used in both fixed-speed and variable-frequency drive (VFD) applications. Variable voltage and variable frequency drives are also used in variable-speed service.

In both induction and synchronous motors, the AC power supplied to the motor's stator creates a magnetic field that rotates in time with the AC oscillations. Whereas a synchronous motor's rotor turns at the same rate as the stator field, an induction motor's rotor

rotates at a slower speed than the stator field. The induction motor stator's magnetic field is therefore changing or rotating relative to the rotor. This induces an opposing current in the induction motor's rotor, in effect the motor's secondary winding, when the latter is short-circuited or closed through external impedance. The rotating magnetic flux induces currents in the windings of the rotor; in a manner similar to currents induced in a transformer's secondary winding(s). The currents in the rotor windings in turn create magnetic fields in the rotor that react against the stator field. Due to Lenz's Law, the direction of the magnetic field created will be such as to oppose the change in current through the rotor windings. The cause of induced current in the rotor windings is the rotating stator magnetic field, so to oppose the change in rotor-winding currents the rotor will start to rotate in the direction of the rotating stator magnetic field. The rotor accelerates until the magnitude of induced rotor current and torque balances the applied load. Since rotation at synchronous speed would result in no induced rotor current, an induction motor always operates slower than synchronous speed. The difference, or "slip," between actual and synchronous speed varies from about 0.5 to 5.0% for standard Design B torque curve induction motors. The induction machine's essential character is that it is created solely by induction instead of being separately excited as in synchronous or DC machines or being self-magnetized as in permanent magnet motors.

For rotor currents to be induced the speed of the physical rotor must be lower than that of the stator's rotating magnetic field ( $n_s$ ); otherwise the magnetic field would not be moving relative to the rotor conductors and no currents would be induced. As the speed of the rotor drops below synchronous speed, the rotation rate of the magnetic field in the rotor increases, inducing more current in the windings and creating more torque. The ratio between the rotation rate of the magnetic field induced in the rotor and the rotation rate of the stator's rotating field is called slip. Under load, the speed drops and the slip increases enough to create sufficient torque to turn the load. For this reason, induction motors are sometimes referred to as asynchronous motors. An induction motor can be used as an induction generator, or it can be unrolled to form a linear induction motor which can directly generate linear motion.

### Synchronous Speed:

The rotational speed of the rotating magnetic field is called as synchronous speed.

$$N_s = \frac{120 \times f}{P} \quad (\text{RPM}) \quad (21)$$

Where,  $f$  = frequency of the supply  
 $P$  = number of poles

**Slip:**

Rotor tries to catch up the synchronous speed of the stator field, and hence it rotates. But in practice, rotor never succeeds in catching up. If rotor catches up the stator speed, there won't be any relative speed between the stator flux and the rotor, hence no induced rotor current and no torque production to maintain the rotation. However, this won't stop the motor, the rotor will slow down due to lost of torque, and the torque will again be exerted due to relative speed. That is why the rotor rotates at speed which is always less the synchronous speed. The difference between the synchronous speed ( $N_s$ ) and actual speed ( $N$ ) of the rotor is called as slip.

$$\% \text{ slip } s = \frac{N_s - N}{N_s} \times 100 \quad (22)$$

**VI. MATLAB/SIMULINK RESULTS**

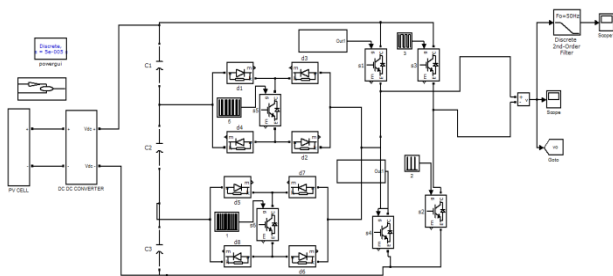


Fig.6 PV system with Single phase Seven level inverter

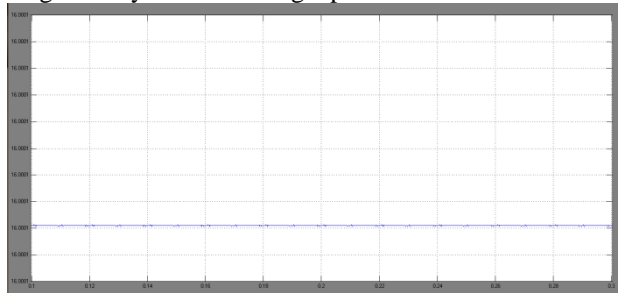


Fig.7 PV system voltage

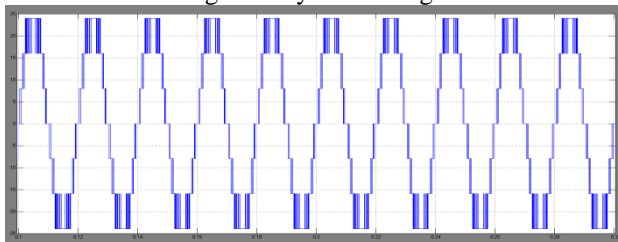


Fig.8 Output Voltage

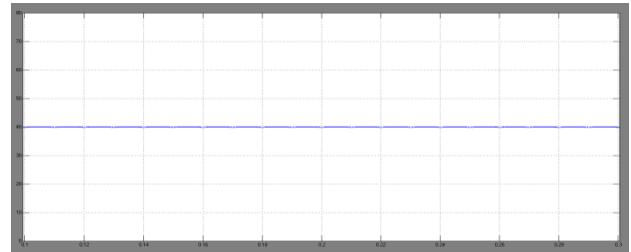


Fig.9 DC Voltage

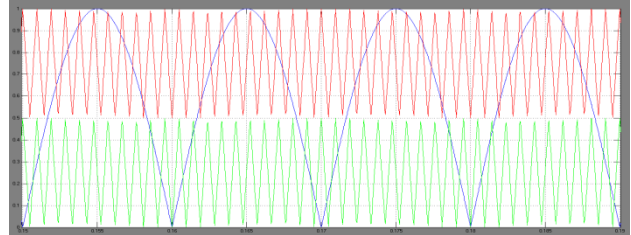


Fig.10 PWM switching signal generation

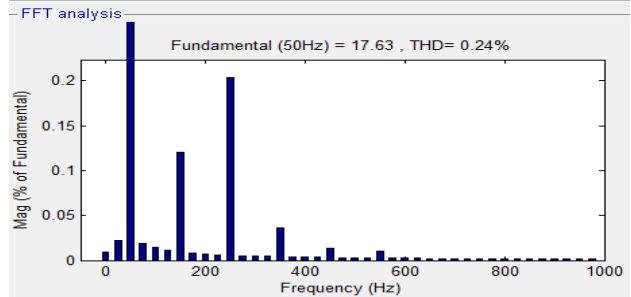
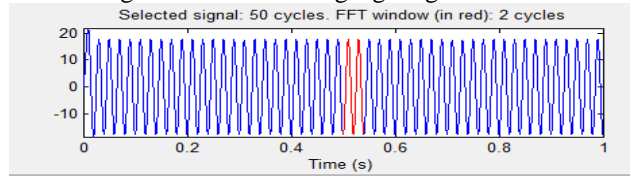


Fig.11. THD result for Single phase seven level of output voltage

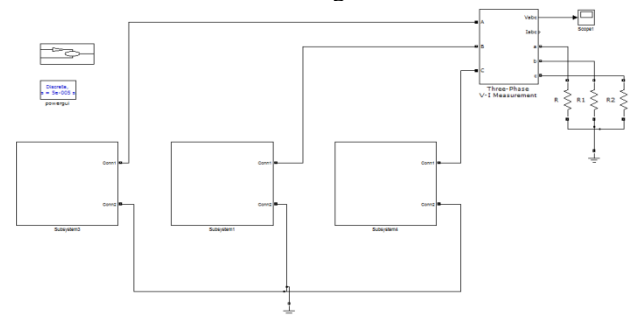


Fig.11 PV system with Three phase Seven level inverter

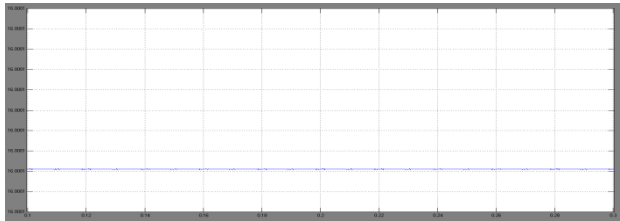


Fig.12 PV system voltage

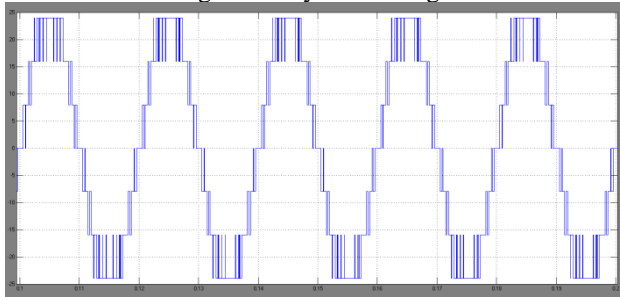


Fig.13 Output Voltage

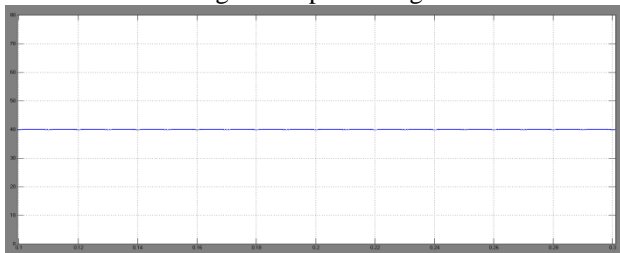


Fig.14 DC Voltage

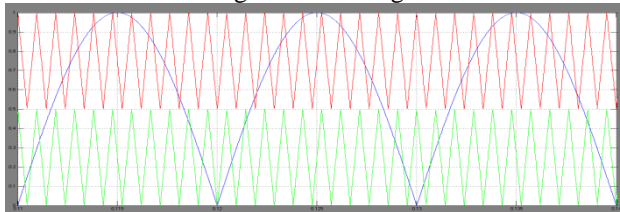


Fig.15 PWM switching signal generation

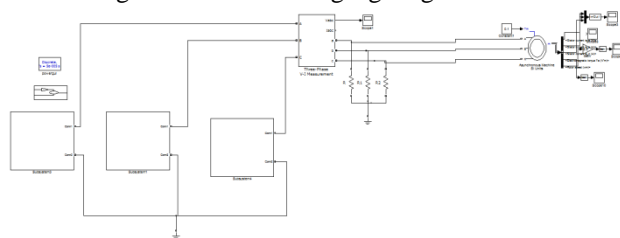


Fig.16 PV system with Three phase Seven level inverter fed Induction Motor Drive

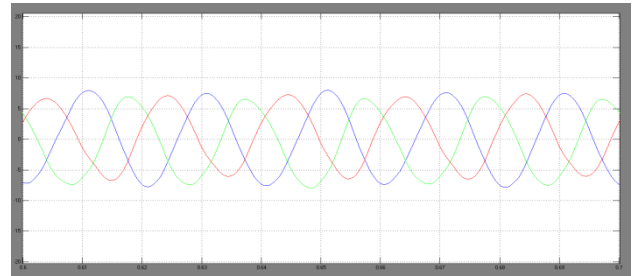


Fig.17 Stator Currents

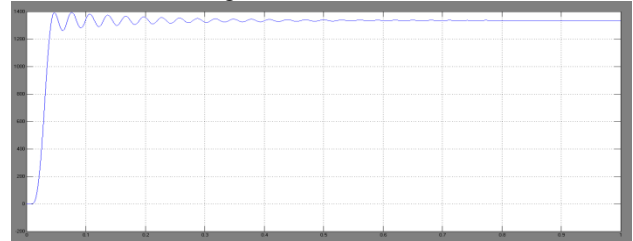


Fig.18 Speed of the Motor

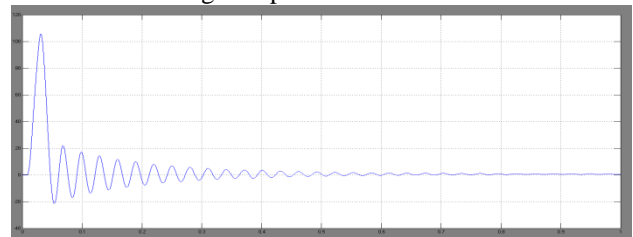


Fig.19 Torque characteristics of the motor

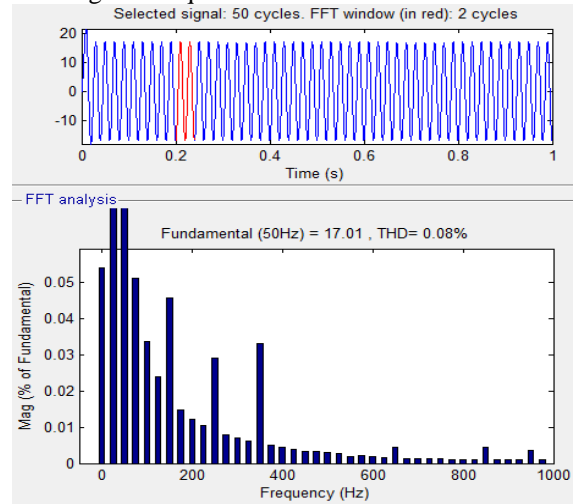


Fig.11. THD result for Single phase seven level of output voltage

## VII. CONCLUSION

This paper presents a new three phase seven level inverter with reduced switches compare to common multi level inverter. Multilevel inverters offer improved output waveforms and lower THD. In this topology less

THD in the three phase seven-level inverter compared with that in the seven-level inverters is connected PV inverters. This inverter provided to induction motor with smooth output and better voltage. Switching loss reduce in this topology than the common three phase multi-level inverter.

#### REFERENCES

- [1] S. Alepuz, S. Busquets-Monge, J. Bordonau, J. Gago, D. Gonzalez, and J. Balcells, —Interfacing renewable energy sources to the utility grid using a three-level inverter, IEEE Trans. Ind. Electron., vol. 53, no. 5, pp. 1504–1511, Oct. 2006
- [2] Sachin Jain and Vivek Agarwal, —A single stage Grid connected inverter topology for solar PV systems with Maximum Power Point Tracking, IEEE Transactions on Power Electronics, vol. 22, issue. 5, Publication year: 2007.
- [3] Shagar Banu M, Vinod S, Lakshmi. S, —Design of DC-DC converter for hybrid wind solar energy system, 2012 International conference on Computing, Electronics and Electrical Technologies.
- [4] Thanujkumar. Jala, G. Srinivasa Rao, —A novel nine level grid connected inverter for photovoltaic system, International journal of modern Engineering Research, vol. 2, issue. 2, March-April 2012, Page(s): 154-159
- [5] J. Rodríguez, J. S. Lai, and F. Z. Peng, —Multilevel inverters: A survey of topologies, controls, and applications, IEEE Trans. Ind. Electron., vol. 49, no. 4, pp. 724–738, Aug. 2002
- [6] S. A. Khajehoddin, A. Bakhshai, P. Jain, —The Application of the Cascaded Multilevel Converters in Grid Connected Photovoltaic Systems, IEEE Canada Electrical Power Conference, 25-26 Oct. 2007, pp. 296-301
- [7] S. B. Kjaer, J. K. Pedersen, and F. Blaabjerg, —A review of single phase grid connected inverters for photovoltaic modules, IEEE Trans. Ind. Appl., vol. 41, no. 5, pp. 1292–1306, Sep./Oct. 2000.
- [8] L. M. Tolbert, F. Z. Peng, —Multilevel Converters as a Utility Interface for Renewable Energy Systems, IEEE Power Engineering Society Summer Meeting, Seattle, Washington, July 15-20, 2000, pp. 1271-1274
- [9] M. Calais and V. G. Agelidis, —Multilevel converters for single-phase grid connected photovoltaic systems—An overview, in Proc. IEEE Int. Symp. Ind. Electron., 1998, vol. 1, pp. 224–229.
- [10] Faete Filho, Yue cao, Leon M. Tolbert, —11 level cascaded H bridge grid tied inverter interface with solar panels, Publication year: 2010